

**Fourier Transform Infrared Emission and Rotational Spectra of the  $X^2\Sigma^+$  states  
of Sr I and Sr II**<sup>1</sup>

C. I. Frum<sup>2</sup>, J. J. Oh<sup>2</sup>, E. A. Cohen and H. M. Pickett

Jet Propulsion Laboratory

*California Institute of Technology*

*Pasadena, California 91109*

<sup>1</sup> This research was performed at the Jet Propulsion Laboratory, California Institute of Technology, under the contract with the National Aeronautics and Space Administration.

<sup>2</sup> NASA-National Research Council Resident Research Associates.

## ABSTRACT

The vibration-rotation spectrum of the  $^2\Sigma^+$  ground state of strontium monohydride has been recorded in emission using a Fourier transform spectrometer. The rotational spectra of  $\text{SrH}$  and  $\text{SrD}$  have also been measured between 200 GHz and 450 GHz using an absorption spectrometer. The gas phase free radicals have been produced in a ceramic furnace by the reaction of elemental strontium with molecular hydrogen or deuterium in the presence of a high voltage electrical discharge. The molecular constants including the rotational constant, centrifugal distortion constants, spin-rotation constants, and magnetic hyperfine interaction constants have been determined from the spectra.

## INTRODUCTION

The diatomic metal hydrides have contributed significantly to better understanding of chemical bonding because of their susceptibility to detailed higher level molecular calculations. Among these species, the monohydrides of the alkaline-earth metals have received considerable attention both from the experimentalists and the theoreticians. The monohydrides of Mg, Ca, Sr, and Ba are relatively easy to synthesize in the gas-phase and have interesting  $^2\Sigma^+$  ground states. Additionally, some of these molecular species (MgH and CaH) are important astrophysical molecules [1-2] and their presence has been detected in the Sun and other stars [3-6].

In the laboratory, the hydrides of alkaline-earth metals have been intensively examined through their optical spectra [7-11]. The ESR spectra of these species trapped in solid inert gases at 4 K have also been investigated by Knight *et al* [12]. Recently, the gas-phase vibration-rotation spectra of these free radicals have been recorded both using diode lasers [8,9,11] and Fourier transform spectrometers [13,14]. However, the gas-phase rotational spectra have been recorded only for the monohydrides of Mg and Ca [15-17]. In the present study we investigated the rotational spectra of  $^{88}\text{SrH}$  and  $^{88}\text{SrD}$  and their isotopomers. SrH has large hyperfine splittings which allow the determination of the Fermi contact,  $A_{iso}$ , and spin dipolar,  $A_{dip}$ , hyperfine parameters.

The first observation of SrH was reported more than sixty years ago by Watson and Fredrikson [18] who analyzed the (0,0) and (1,1) bands of the  $A^2\Pi - X^2\Sigma^+$  electronic system. In the last decade, the  $A^2\Pi - X^2\Sigma^+$  and the  $B^2\Sigma^+ - X^2\Sigma^+$  systems were reinvestigated at higher resolution by Appelblad *et al* [19] using a Fourier transform spectrometer. Additionally, the rotation-vibration spectra of the  $^2\Sigma^+$  ground states of the SrH and SrD were measured by Magg *et al* [11] and by Birk *et al* [20].

## EXPERIMENTAL

The rotation-vibration emission spectrum of SrII has been observed using a high-resolution Bruker 1 FS120 spectrometer. The instrument was slightly modified to allow spectral measurement in emission. A 90°, off-axis parabolic mirror (focal length = 6 in) was placed above the alignment port in the source compartment of the spectrometer. This mirror was used to collect the molecular emission from the hot cell where the free radicals have been produced.

The gas phase **SrII** was produced in a similar  $Al_2O_3$  ceramic tube furnace used previously to record the vibration-rotation and rotational spectra of CaII and CaD [14,16]. The free radical was generated at high temperatures by the reaction of metal vapor and molecular hydrogen in an electrical discharge.

About 6 grams of elemental strontium (Johnson Matthey, 99.99% purity) were placed in the middle of the 90 cm long, 5.0 cm diameter ceramic furnace. A quartz liner was used to separate the molten metal and the alumina walls of the furnace. The metal was slowly heated while pumping to remove the impurities. The temperature was monitored with a Pt thermocouple placed between the ceramic tube and the heating elements. When the temperature reached 630°C the pump was valved down and a mixture of argon gas and molecular hydrogen was allowed into the cell. A small flow of Ar/H<sub>2</sub> mixture was maintained in order to prevent the buildup of undesirable impurities.

A DC electrical discharge was generated in the mixture between water cooled electrodes placed at both ends of the tube. As in the case of CaII [14] no molecular signal could be observed without the discharge. However the signal was stronger than the CaII signal probably because the SrH<sub>2</sub> which also form in the reaction is less stable than the calcium equivalent and more easily reduced to SrII.

The unapodized resolution of the spectrometer was 0.0056 cm<sup>-1</sup>. A KBr beam-splitter and a B:Si liquid helium cooled detector were used. The spectral bandpass was limited to

800-1450  $\text{cm}^{-1}$  with an optical filter placed in the detector dewar. The bad fringing caused by the unwedged filter limited the "useful" portion of the spectrum to 918-1400  $\text{cm}^{-1}$ . Numerous spectra were recorded while trying to optimize the conditions of the system to maximize the molecular signal. Between 630°C and 730°C the pressure in the cell dropped rapidly and more hydrogen gas had to be added to maintain the pressure constant suggesting that solid  $\text{SrH}_2$  was formed. The formation of the solid was avoided by maintaining the temperature of the furnace above 750°C. The best spectrum was recorded at 850°C and 4.5 torr. Under these conditions a 4000 V/280 nA electrical discharge remained stable for many hours. At higher temperatures the emission signal from  $\text{SrII}$  diminished considerably and disappeared completely above 900°C.

A total of 400 scans were recorded for the best signal-to-noise ratio. We choose to use a lower spectral resolution in order to obtain the highest signal-to-noise possible. A signal-to-noise ratio of 35:1 for the strongest lines of the R-branch of the fundamental band was obtained. Figure shows a portion of the rotation-vibration spectrum of  $\text{SrII}$ . The emission lines of the free radical appear on the top of the black-body curve of the hot furnace. An expanded portion of the spectrum is shown in Figure II.

The calibration of the spectrum was carried out using water absorption lines which appeared in the same spectrum. The measured lines were calibrated against the frequencies measured by R. A. Toth [21].

The rotational spectra of  $\text{SrII}$  and  $\text{SrI}$  were recorded in absorption using a millimeter spectrometer similar to that described by Birk *et al.* [22] and modified as described in Ref. [16]. The second through the fifth harmonics of a 07- GHz klystron were used to cover the frequency range 214-443 GHz.

The free radicals were produced in the same ceramic furnace used to record the rotation vibration spectrum of  $\text{SrII}$ . The best results were obtained at a temperature of 750°C, 40 torr total pressure and a discharge current of 280 nA at 3500 V. Under these conditions the

electrical discharge was very stable allowing sufficient spectral integration to obtain a better than 65:1 signal-to-noise ratio for the strongest lines. A portion of the rotational spectrum **Sri]** is shown in Figure III. The well resolved molecular transitions of **Sri]** are 2-2.5 MHz wide with Doppler and pressure broadening equally contributing to the line widths. For the purpose of the fit an uncertainty of 150 kHz was assigned to each rotational line.

## DISCUSSION

The spectral analysis of the infrared spectrum was carried out using PC-DECOMP, a spectral analysis program developed by J. W. Brault of the National Solar Observatory at Kitt Peak. The rovibrational line profiles were fitted to Voigt line shape functions. The larger coverage available with the FTS allowed the measurement of a larger number of vibration-rotation lines in both the P- and R-branches. However, due to the sensitivity of our instrument, the data set is limited only to the strongest fundamental band and to  $J$ -values lower than 20. The measured vibration-rotation transitions of SrH are given in Table 1. The molecular constants were extracted by least-squares analysis using SPFIT, a spectrum fitting and predicting program written by H.M. Pickett [23]. The rotational transitions were predicted using these constants and the hyperfine constants measured by Knight et al [12] on matrix isolated SrH. Using the prediction the hyperfine components of the  $N=2-1$ ,  $N=1-0$  transitions of the  $v=0$  and  $v=1$  states of  $^{88}\text{SrH}$ , and the  $N=2-1$  of the  $v=0$  state of the  $^{86}\text{SrH}$  could be readily measured. The blended features for the  $AT=3-2$ ,  $N=3-4$ , transitions of  $v=0$  and  $v=1$  states  $^{88}\text{SrD}$  and  $N=3-2$ ,  $N=3-4$  transitions of the  $v=0$  and  $v=1$  states of  $^{86}\text{SrD}$  were also measured. Sri] data consist of three kinds of transitions. The  $\Delta P = \Delta J = 1$  transitions are the strongest and appear well resolved in both  $N=1-0$  and  $N=2-1$  transitions. The  $\Delta P = \Delta J = 0$  and  $\Delta P = 0, \Delta J = 1$  transitions are also resolved but their intensity diminishes and the weakest three transitions could not be reliably measured. The observed Sri) transitions appear as partially resolved or unresolved triplets with  $\Delta N = \Delta J = 1$ . Therefore, the reported SrD frequencies are given as the center of the blended multiplet. The measured rotational transitions for  $^{88}\text{SrH}$  and  $^{86}\text{SrH}$  listed together with their assignment are shown in Table 11.  $^{88}\text{SrD}$  and  $^{86}\text{SrD}$  lines are listed in Table III together with the calculated frequencies of the hyperfine components of each measured line and the weighted average of the unresolved hyperfine multiplet.

The data were analyzed using the Hamiltonian for a Hund's case (b)  $^2\Sigma^+$  molecule with nuclear spin, I. The case  $b_{\beta J}$  for the nuclear spin coupling, was assumed.

$$\begin{aligned}\mathbf{H} &= \mathbf{H}_{rfs} + \mathbf{H}_{hfs} \\ \mathbf{H}_{rfs} &= B\mathbf{N}^2 + D\mathbf{N}^4 + \{H\mathbf{N}^6 + (\gamma + \gamma_D\mathbf{N}^2)\mathbf{N} \cdot \mathbf{S}\} \\ \mathbf{H}_{hfs} &= A_{iso}\mathbf{I} \cdot \mathbf{S} + A_{dip}[3I_zS_z - \mathbf{I} \cdot \mathbf{S}] + C_I\mathbf{I} \cdot \mathbf{S}\end{aligned}$$

where  $B$ ,  $D$ ,  $H$ ,  $\gamma$ , and  $\gamma_D$  are the rotational, quartic and sextic centrifugal distortion, and spin-rotation interaction constants. The hyperfine interaction is expressed as the sum of the isotropic and dipolar spin-spin, and nuclear spin-rotation interaction contributions. The value of  $C_I$  is not determined from the data and the nuclear spin-rotation term was excluded from the fits. The data do however allow an upper limit of  $\leq 100$  kHz to be placed on the magnitude of the nuclear spin-rotation interaction constant.

The  $^{88}\text{SrII}$  vibration-rotation and rotational data were fitted together. The standard deviation of the fit was about 100 kHz, slightly smaller than the 150 kHz experimental error of the rotational lines. The  $^{88}\text{SrD}$  rotational data was fitted together with the diode laser vibrational data of Birk et al. [20]. The Fermi contact and the dipolar interaction terms were fixed to the values calculated from constants of SrII using the isotope relationships  $([A_{iso}, A_{dip}]_D = I_H/I_D\mu_D/\mu_H[A_{iso}, A_{dip}]_H)$ . These constants together with the rotational, centrifugal distortion, and spin-rotation interaction constants of SrI and SrD main isotopomers are also shown in Table IV. For the minor isotopomers  $^{86}\text{SrII}$  and  $^{86}\text{SrI}$  only few rotational transitions could be measured. The data was fitted keeping all the constants except the rotational constant fixed to the values determined from the constants of the main isotopomer using the isotope relationships.

The gas phase value of the Fermi contact constant,  $A_{iso}$  is 24 MHz larger than the argon matrix value of 122 MHz. The same trend is observed in MgII and CaII where the difference



between the gas phase and the matrix values of the isotropic constant increases also. This is expected since as the metal atom becomes heavier the spin density on the metal atom increases and the bonding becomes more ionic. The dipolar interaction constant,  $A_{dip}$  is more than twice the matrix value of 0.6 MHz. This is different from MgII and CaII where the difference between the gas-phase value and matrix value is negligible.

We also calculated the line intensity,  $I_{fi}(T)$ , for the low- $N$  rotational transitions of  $^2\Sigma^+$  ground states of  $^{88}\text{SrII}$  and  $^{88}\text{SrI}$  according to

$$I_{fi}(T) = (8\pi/3hc)\nu_{fi}S_{fi}\mu_z^2[e^{-E''/kT} - e^{-E'/kT}]/Q_{rs}$$

where  $\nu_{fi}$ ,  $S_{fi}$ ,  $\mu_z$ ,  $E''$ ,  $E'$ , and  $Q_{rs}$  are the transition frequency, line strength, the component of the dipole moment along the internuclear axis, lower and upper state energies and the rotation-spin partition function, respectively. The rotational line strengths, the energies, and the line intensity (reported as  $\log(I_T)$ ), calculated for  $\mu_z = 1D$  and  $T = 3001K$  are given in Tables V and VI. The uncertainty for the frequency (listed in parentheses) is an estimate of the calculated uncertainty based on the linearized least square fit.

## ACKNOWLEDGMENTS

This research was performed at the Jet Propulsion Laboratory, California Institute of Technology, under contract with the National Aeronautics and Space Administration. C.I.F. and J.J. O. thank the National Research Council for NRC-NASA Resident Research Associateship during this research.

## REFERENCES

1. P. F. Bernath, J. H. Black, J. W. Brault, *Astrophys. J.*, 298, 375-381 (1985).
2. M. Oppenheimer and A Dalgarno, *Astrophys. J.*, 192, 232 (1974).
3. P. Sotirovski, *Astr. Ap. Suppl.*, 6, 85 - 88 (1972).
4. C. M. Olmstedt, *Astrophys. J.*, 27, 66-69 (1908).
5. A. Eagle, *Astrophys. J.*, 30, 231-236 (1909).
6. Y. Öhman, *Stockholm Obs. Ann.*, 12, 3-20 (1935).
7. H. Martin, *J. Chem. Phys.*, 88, 1797-1806 (1988).
8. B. Lemoine, C. Demuynck, J. L. Destombes and P. B. Davis, , 151, 263-266 (1988).
9. J. Petitprez, B. Lemoine, C. Demuynck, J. L. Destombes, B. Macke,  
*J. Chem. Phys.*, 91, 4462-4467 (1989).
10. O. Appelblad, L. E. Berg, J. Klynning, and J. W. C. Johns,  
*Phys. Scripta*, 31, 69-73 (1985).
11. U. Magg, H. Birk, and H. Jones, *Chem. Phys. Lett.*, 149, 321-325 (1988).
12. Knight, L. B. Jr., and Weltner, W. Jr. 1971, *J. Chem. Phys.*, 54, 3875-3884 (1971)
13. K. A. Walker, H. G. Hedderich, P. F. Bernath, *Mol. Phys.*, 78, 577-589 (1993).
14. C. I. Frum and H. M. Pickett, *J. Mol. Spec.*, 159, 329-336 (1993).
15. R. Zink, J. A. Jennings, K. M. Evenson, and K. J. Leopold,  
*Astrophys. J.*, 359, 65-66 (1990).
16. W. L. Barklay, M. A. Anderson, L. M. Ziurys, *Astrophys. J.*, 408, 65-67 (1993)

17. C. 1. Frum, J. J. Oh, E. A. Cohen, and H. M. Pickett, *Astrophys. J. Letters*,  
408, 61-64(1993).
18. W. W. Watson and W. R. Friedrikson, *Phys. Rev.*, 39, 765-776(1932).
19. O. Appelblad, L. Klymning and J. W. C. Johns, *Phys. Scripta*, **33**, 415-419(1986).
20. H. Birk, R. D. Urban, L. Polonsky, and H. Jones, *J. Chem. Phys.*, 94, 5435-5442(1991).
21. R. A. Toth, *J. Opt. Soc. B*, 8, 2236-2255(1991).
- X?.. M. Birk, R. R. Friedel, E. A. Cohen, and H. M. Pickett, *J. Chem. Phys.*,  
**91**, 6588-6597(1989).
23. H. M. Pickett, *J. Mol. Spectrosc.*, 148, 371-377(1991),

Table . Measured ro-vibrational transitions of SrII ( $cm^{-1}$ ).

$N'$	$v'$	$J'$	$N''$	$v''$	$J''$	Transition	$\sigma$ - c.
2	1	1.5	3	0	2.5	1150.60372	0.00079
2	1	2.5	3	0	3.5	1150.46819	-0.00046
3	1	2.5	4	0	3.5	1142.87650	0.00010
3	1	3.5	4	0	4.5	1142.73867	0.00029
4	1	3.5	5	0	4.5	1135.00192	-0.00045
4	1	4.5	5	00	5.5	1134.86129	0.00069
5	1	4.5	6	0	5.5	1126.98357	-0.00048
5	1	5.5	6	00	6.5	1126.83825	-0.00033
6	1	5.5	7	00	6.5	1118.82505	0.00037
6	1	6.5	7	00	7.5	1118.67489	-0.00066
7	1	6.5	8	0	7.5	1110.52803	0.00055
7	1	7.5	8	0	8.5	1110.37552	0.00076
8	1	7.5	9	0	8.5	1102.09514	-0.00053
8	1	8.5	9	0	9.5	1101.93917	-0.00025
9	1	8.5	10	0	9.5	1093.53209	-0.00035
9	1	9.5	10	000	11	1093.37284	0.00011
10	1	9.5	11	00	11	1084.84053	-0.00046
10	1	11	11	00	12	1084.67828	0.00041
11	1	11	12	0	12	1076.02374	-0.00072
11	1	12	12	0	13	1075.85838	0.00037
12	1	12	13	0	13	1067.08524	-0.00077
12	1	13	13	0	14	1066.91606	-0.00024
13	1	13	14	0	14	1058.02908	0.00033
13	1	14	14	0	15	1057.85499	-0.00085
14	1	14	15	0	15	1048.85547	-0.00030
14	1	15	15	0	16	1048.67924	-0.00048
15	1	16	16	0	17	1039.39136	0.00035
16	1	16	17	0	17	1030.17511	0.00028
16	1	17	17	0	18	1029.99244	-0.00028
17	1	17	18	0	18	1020.67277	-0.00012
17	1	18	18	0	19	1020.48928	0.00143
18	1	18	19	0	19	1011.06376	-0.00349
18	1	19	19	00	20	1010.87852	-0.00082
19	1	19	20	00	20	1001.36097	0.00015
19	1	20	20	00	21	1001.17021	0.00010

Table 1. Measured ro-vibrational transitions of SrII ( $\text{cm}^{-1}$ ).

$N'$	$v'$	$J'$	$N''$	$v''$	$J''$	Transition	$\sigma$ -c.
3	1	2.5	2	0	1.5	1193.57150	-0.00008
3	1	3.5	2	0	2.5	1193.68140	0.00029
4	1	3.5	3	0	2.5	1200.17953	0.00088
4	1	4.5	3	0	3.5	1200.28447	0.00075
5	1	4.5	4	0	3.5	1206.61244	0.00016
5	1	5.5	4	0	4.5	1206.71260	-0.00028
6	1	5.5	5	0	4.5	1212.87035	0.00106
6	1	6.5	5	0	5.5	1212.96381	-0.00158
7	1	6.5	6	0	5.5	1218.94528	-0.00124
7	1	7.5	6	0	6.5	1219.03719	-0.00086
8	1	7.5	7	0	6.5	1224.84024	-0.00056
8	1	8.5	7	0	7.5	1224.92835	0.00065
9	1	8.5	8	0	7.5	1230.55000	0.00101
9	1	9.5	8	0	8.5	1230.63170	0.00049
10	1	9.5	9	0	8.5	1236.06958	0.00158
10	1	11	9	0	9.5	1236.14336	-0.00210
11	1	11	10	0	9.5	1241.39529	0.00056
11	1	12	10	0	11	1241.46631	-0.00106
12	1	12	11	0	11	1246.52573	-0.00041
12	1	13	11	0	12	1246.59648	0.00259
13	1	13	12	0	12	1251.45977	0.00056
13	1	14	12	0	13	1251.52136	-0.00064
14	1	14	13	0	13	1256.19034	-0.00061
14	1	15	13	0	14	1256.24815	-0.00057
15	1	15	14	0	14	1260.71791	-0.00051
15	1	16	14	0	15	1260.77240	0.00129
16	1	16	15	0	15	1265.03715	-0.00158
16	1	17	15	0	16	1265.08804	0.00178
17	1	17	16	0	16	1269.14876	-0.00024
17	1	18	16	0	17	1269.19091	-0.00040
18	1	18	17	0	17	1273.04559	-0.00085
18	1	19	17	0	18	1273.08389	0.00044
19	1	19	18	0	18	1276.72936	0.00110
19	1	20	18	0	19	1276.75951	-0.00041

Table 1. Measured rotational transitions of  $^{88}\text{SrII}$  and  $^{86}\text{SrII}$ . ( $MHz$ ).

$N'$	$v'$	$J'$	$J''$		$v''$	$J''$	$J'''$		$J_{\text{Exp.}} J_{\text{req}}$	$\text{o.-c.}$
$^{88}\text{SrII}$										
1	0	0.5	1	0	0	0.5	1		214073.981	0.049
1	0	1.5	2	0	0	0.5	1		219697.666	0.148
2	0	1.5	1	1	0	0.5	1		433773.745	-0.024
2	0	1.5	2	1	0	0.5	1		433715.821	-0.004
2	0	1.5	1	1	0	0.5	0		433725.964	-0.015
2	0	2.5	3	1	0	1.5	2		437438.257	-0.015
2	0	2.5	2	1	0	1.5	1		437447.792	-0.019
2	0	2.5	2	1	0	1.5	2		437351.554	-0.044
2	1	1.5	1	1	1	0.5	1		424213.787	-0.009
2	1	1.5	2	1	1	0.5	1		424152.706	0.026
2	1	1.5	1	1	1	0.5	0		424163.368	-0.007
2	1	2.5	3	1	1	1.5	2		427752.310	-0.036
2	1	2.5	2	1	1	1.5	1		427762.414	0.038
$^{86}\text{SrII}$										
2	1	2.5	2	1	1	1.5	2		437552.720	0.0140
2	1	2.5	1	1	1	1.5	1		437562.235	-0.0140

**Table 111. Measured relational transitions of SrD(Mhz).**

<i>N'</i>	<i>J'</i>	<i>I'</i>	<i>N''</i>	<i>J''</i>	<i>I''</i>	Exp. Freq,	Avg. calc.	o.-c..	(Lit.) r('q
<sup>88</sup> SrD									
3	3.5	4.5	2	2.5	3.5	332925.122			332925.174
3	<b>3.5</b>	<b>3.5</b>	2	2.5	2.5	332926.526	332926.472	0.054	332926.463
<b>3</b>	<b>3.5</b>	<b>2.5</b>	2	2.5	1.5				332926.484
4	3.5	3.5	3	2.5	2.5				441582.391
4	3.5	4.5	3	2.5	3.5	441582.554	441582.554	0.000	441582.377
4	3.5	2.5	3	2.5	1.5				441583.111
4	4.5	5.5	3	3.5	4.5				443467.860
4	4.5	4.5	3	3.5	3.5	443468.281	443468.282	-0.002	443468.576
4	4.5	3.5	3	3.5	2.5				443468.587
4	4.5	5.5	3	3.5	4.5				436518.508
4	4.5	4.5	3	3.5	3.5	436518.855	436518.931	-0.076	436519.224
4	4.5	3.5	3	3.5	2.5				436519.235
<sup>86</sup> SrD									
3	3.5	4.5	2	2.5	3.5	333097.591			333097.712
3	3.5	3.5	2	2.5	2.5	333098.784	333099.0170	0.226	332926.463
3	3.5	2.5	2	2.5	1.5				332926.484
4	4.5	5.5	3	3.5	4.5				443697.637
4	4.5	4.5	3	3.5	3.5	443697.954	443698.059	-0.105	443698.353
4	4.5	3.5	3	3.5	2.5				443698.364



**Table IV. Molecular constants of  $^{88}\text{SrH}$  and  $^{88}\text{SrD}$  (in MHz).**

Constant	$\text{s}[\text{MHz}]$	$\text{SrD}$
$B_0$	108927.8503(149) <sup>a</sup>	55349.1082(302)
$D_0$	4.06069(133)	-1.04550(93)
$H_0 \times 10^5$	10.60(27)	0.1378 <sup>c</sup>
$\gamma_0$	3717.062(94)	1888.012(174)
$\gamma_{D,0}$	-0.3365(99) <sup>b</sup>	0.0863 <sup>d</sup>
$A_{\text{iso}}$	146.1159(201)	22.773 <sup>d</sup>
$A_{\text{dip}} \times 3$	4.04(40)	0.625 <sup>d</sup>
$v_1$	35159841.6(4.7)	25229832.5(72)
$B_1$	106521.7245(171) <sup>a</sup>	54483.173(26)
$D_1$	4.054022(131) <sup>b</sup>	1.04428(93) <sup>c</sup>
$\gamma_1$	3593.800(153)	1844.4787(174)
$A_{\text{iso},1}$	154.10(66)	22.77 <sup>d</sup>
$A_{\text{r(ii.)}} \times 3$	4.37(59)	0.625 <sup>d</sup>

a. One standard deviation is included in parentheses

b. Common for both vibrational states

c. Fixed to the values calculated from the Dunham's Y's of Ref [18]

d. Fixed to the values calculated from the  $^{88}\text{SrH}$  constants using isotope relationships.

Table V. Line intensities of the low-  $N$  rotational transitions of  $X^2\Sigma^+$  state of SrII.

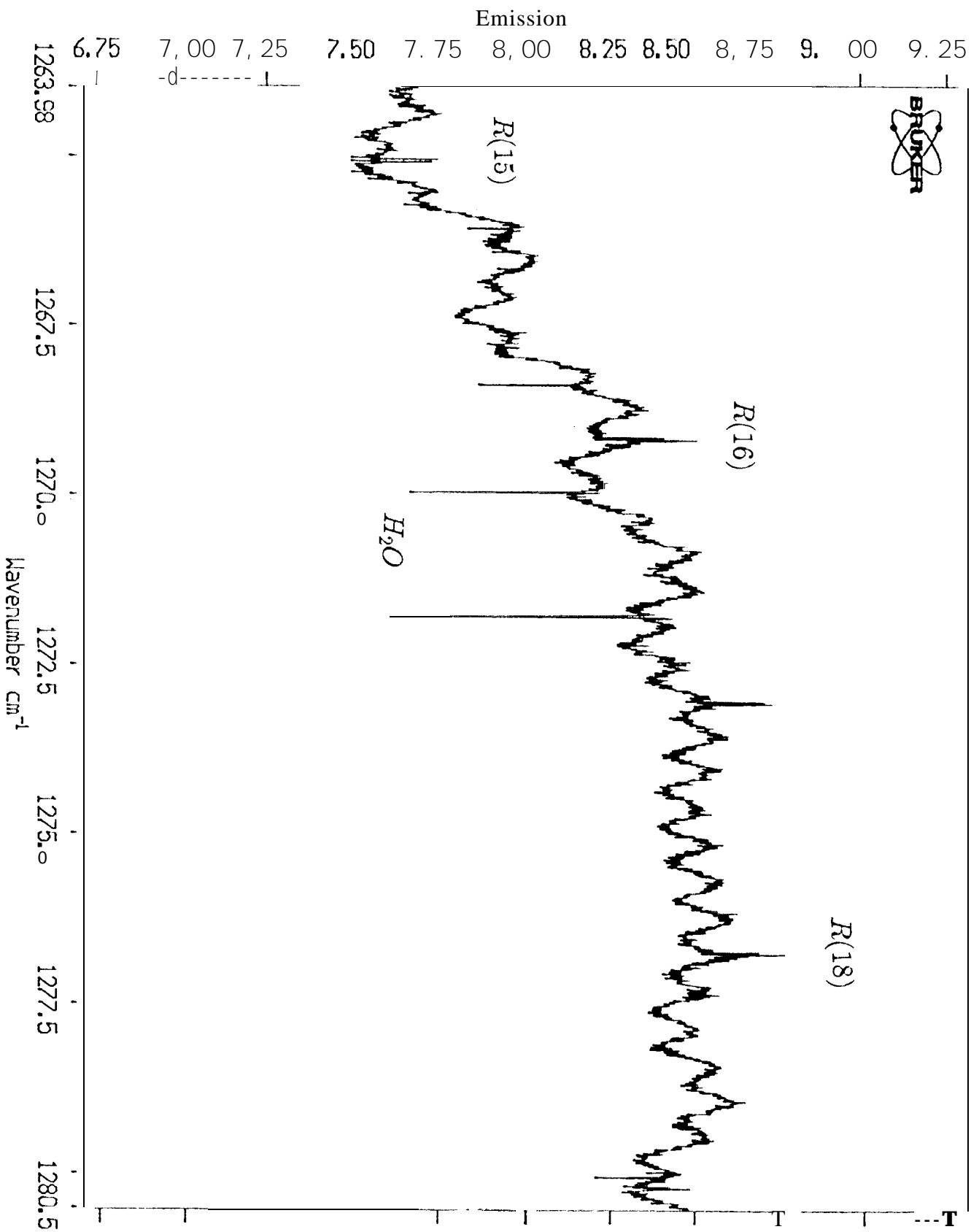
Freq( $1\sigma$ unc.)/MHz	Line Str.	$\log(I_{300})$	$E/\text{cm}^{-1}$	$N'$	$J'$	$P'$	$N''$	$J''$	$P''$
214073.932( 85)	0.6548	-3.0720	0.0049	1	0.5	1	0	0.5	1
214121.722(158)	0.3333	- 3.3651	0.0049	1	0.5	0	0	0.5	1
214220.091(198)	0.3452	-3.3405	0.0000	1	0.5	1	0	0.5	0
219601.306(125)	0.3452	-3.3281	0.0049	1	1.5	1	0	0.5	1
219697.518( 47)	1.6667	-2.6440	0.0049	1	1.5	2	0	0.5	1
219747.464(102)	0.6548	-3.0495	0.0000	1	1.5	1	0	0.5	0
428092.238(139)	0.2962	- 2.8373	7.3332	2	1.5	2	1	1.5	2
428150.183(148)	0.0333	-3.7858	7.3332	2	1.5	1	1	1.5	2
428188.451(155)	0.0313	-3.8136	7.3300	2	1.5	2	1	1.5	1
428246.395(182)	0.1726	- 3.0715	7.3300	2	1.5	1	1	1.5	1
433715.825( 55)	1.6725	- 2.0739	7.1456	2	1.5	2	1	0.5	1
433725.979( 88)	0.6667	-2.4734	7.1472	2	1.5	1	1	0.5	0
433773.769( 92)	0.3274	-2.7821	7.1456	2	1.5	1	1	0.5	1
437351.598( 91)	0.2038	- 2.9813	7.3332	2	2.5	2	1	1.5	2
437438.272( 58)	2.8000	- 1.8432	7.3332	2	2.5	3	1	1.5	2
437447.811( 66)	1.7961	- 2.0360	7.3300	2	2.5	2	1	1.5	1
442975.184(151)	0.0000	- 6.6200	7.1456	2	2.5	2	1	0.5	1
641925.147(233)	0.1886	-2.7191	21.9246	3	2.5	3	2	2.5	3
641987.269(219)	0.0095	-4.0158	21.9246	3	2.5	2	2	2.5	3
642011.821(214)	0.0088	-4.0478	21.9217	3	2.5	3	2	2.5	2
642073.943(220)	0.1359	- 2.8613	21.9217	3	2.5	2	2	2.5	2
651271.180(139)	2.8025	- 1.5342	21.6128	3	2.5	3	2	1.5	2
651275.358(139)	1.8000	- 1.7265	21.6147	3	2.5	2	2	1.5	1
651333.302(140)	0.1975	- 2.6862	21.6128	3	2.5	2	2	1.5	2
654900.570(138)	0.1447	- 2.8172	21.9246	3	3.5	3	2	2.5	3
654983.169(144)	3.8571	- 1.3913	21.9246	3	3.5	4	2	2.5	3
654987.244(147)	2.8553	-1.5220	21.9217	3	3.5	3	2	2.5	2
664246.603(213)	0.0000	- 6.8154	21.6128	3	3.5	3	2	1.5	2
855473.882(529)	0.1378	-2.6587	43.7725	4	3.5	4	3	3.5	4
855538.305(504)	0.0040	- 4.1993	43.7725	4	3.5	3	3	3.5	4
855556.481(496)	0.0037	-4.2327	43.7697	4	3.5	4	3	3.5	3
855620.904(481)	0.1085	-2.7623	43.7697	4	3.5	3	3	3.5	3
868531.905(321)	3.8585	- 1.1979	43.3360	4	3.5	4	3	2.5	3
868534.205(320)	2.8571	- 1.3284	43.3390	4	3.5	3	3	2.5	2
FJ85W.328(310)	0.1415	- 2.6336	43.3369	4	3.5	3	3	2.5	3
872154.703(315)	0.1122	-2.7318	43.7725	4	4.5	4	3	3.5	4
872235.039(329)	4.8889	- 1.0925	43.7725	4	4.5	5	3	3.5	4
872237.302(330)	3.8878	- 1.1920	43.7697	4	4.5	4	3	3.5	3
885212.726(501)	0.0000	- 6.9895	43.3369	4	4.5	4	3	2.5	3

**Table VI. line intensities of the low-  $N$  rotational transitions of  $X^2\Sigma^+$  state of Sri).**

Freq(1 $\sigma$ unc.)/MHz	Line Str.	$\log(I_{300})$	$E/\text{cm}^{-1}$	$N'$	$J'$	$K'$	$N''$	$J''$	$K''$
108790.149(207)	0.7327	-4.0841	0.0011	1	0.5	1.5	0	0.5	1.5
108801.181(207)	0.5910	-4.1774	0.0011	1	0.5	0.5	0	0.5	1.5
108824.309(207)	0.6006	-4.1702	0.0000	1	0.5	1.5	0	0.5	0.5
108835.340(207)	0.0757	-5.0697	0.0000	1	0.5	0.5	0	0.5	0.5
111608.151(79)	0.0757	-5.0479	0.0011	1	1.5	0.5	0	0.5	1.5
111619.557(79)	0.6006	-4.14s3	0.0011	1	1.5	1.5	0	0.5	1.5
111638.363(79)	2.0000	-3.6257	0.0011	1	1.5	2.5	0	0.5	1.5
111642.311(79)	0.5910	-4.1551	0.0000	1	1.5	0.5	0	0.5	0.5
111653.717(79)	0.7327	-4.0616	0.0000	1	1.5	1.5	0	0.5	0.5
217567.905(402)	0.3334	-3.8356	3.7250	2	1.5	2.5	1	1.5	2.5
217579.105(402)	0.0638	-4.5536	3.7250	2	1.5	1.5	1	1.5	2.5
217586.711(402)	0.0623	-4.5640	3.7244	2	1.5	2.5	1	1.5	1.5
217597.911(402)	0.1456	-4.1954	3.7244	2	1.5	1.5	1	1.5	1.5
217604.658(402)	0.0601	-4.5799	3.7244	2	1.5	0.5	1	1.5	1.5
217609.317(402)	0.0592	-4.5860	3.7240	2	1.5	1.5	1	1.5	0.5
217616.064(402)	0.0757	-4.4793	3.7240	2	1.5	0.5	1	1.5	0.5
220416.118(156)	2.0043	-3.0452	3.6300	2	1.5	2.5	1	0.5	1.5
220416.287(156)	0.7424	-3.4766	3.6304	2	1.5	1.5	1	0.5	0.5
220423.034(156)	0.5910	-3.5756	3.6304	2	1.5	0.5	1	0.5	0.5
220427.319(156)	0.5891	-3.5770	3.6300	2	1.5	1.5	1	0.5	1.5
220434.065(156)	0.0733	-4.4821	3.6300	2	1.5	0.5	1	0.5	1.5
222278.841(93)	0.0162	-5.1310	3.7250	2	2.5	1.5	1	1.5	2.5
222291.190(93)	0.3866	-3.7528	3.7250	2	2.5	2.5	1	1.5	2.5
222298.647(93)	0.3854	-3.7542	3.7244	2	2.5	1.5	1	1.5	1.5
222306.986(93)	3.2000	-2.8349	3.7250	2	2.5	3.5	1	1.5	2.5
222309.996(93)	2.0134	-3.0361	3.7244	2	2.5	2.5	1	1.5	1.5
222310.053(93)	1.1984	-3.3114	3.7240	2	2.5	1.5	1	1.5	0.5
326298.225(579)	0.2087	-3.7063	11.1404	3	2.5	3.5	2	2.5	3.5
326309.456(579)	0.0186	-4.7559	11.1404	3	2.5	2.5	2	2.5	3.5
326314.021(579)	0.0181	-4.7671	1.1398	3	2.5	3.5	2	2.5	2.5
326325.252(579)	0.1353	-3.8945	1.1398	3	2.5	2.5	2	2.5	2.5
326333.298(579)	0.0184	-4.7606	1.1398	3	2.5	1.5	2	2.5	2.5
326336.601(579)	0.0181	-4.7686	1.1395	3	2.5	2.5	2	2.5	1.5
326344.648(579)	0.0971	-4.0383	1.1395	3	2.5	1.5	2	2.5	1.5

**Table VI.** Line intensities of the low-N rotational transitions of  $X^2\Sigma^+$  state of SrD.

Freq(1 $\sigma$ unc. )/MHz	Line Str.	$\log(I_{300})$	$\lambda$ / $\mu$ m	N'	J'	P'	N''	J''	P''
331037.306(160)	3.2018	- 2.5076	10.9823	3	2.5	3.5	2	1.5	2.5
331037.337(160)	2.0171	-2.7083	10.9827	3	2.5	2.5	2	1.5	1.5
331038.637(160)	1.2000	-2.9339	0.9829	3	2.5	1.5	2	1.5	0.5
331045.383(160)	0.3829	-3.4300	0.9827	3	2.5	1.5	2	1.5	1.5
331048.537(160)	0.3824	- 3.4305	0.9823	3	2.5	2.5	2	1.5	2.5
331056.584(160)	0.0159	-4.8122	0.9823	3	2.5	1.5	2	1.5	2.5
332899.331 (91)	0.0059	5.2394	1.1404	3	3.5	2.5	2	2.5	3.5
332910.659(91)	0.2811	- 3.5596	1.1404	3	3.5	3.5	2	2.5	3.5
332915.127(91)	0.2807	- 3.5602	1.1398	3	3.5	2.5	2	2.5	2.5
332925.166(91)	4.2857	- 2.3765	11.1404	3	3.5	4.5	2	2.5	3.5
332926.455(91)	3.1474	- 2.5105	11.1398	3	3.5	3.5	2	2.5	2.5
332926.476(91)	2.2848	-2.6496	11.1395	3	3.5	2.5	2	2.5	1.5
434955.435(736)	0.1502	- 3.6264	22.2455	4	3.5	4.5	3	3.5	4.5
434966.680(736)	0.0078	- 4.9096	22.2455	4	3.5	3.5	3	3.5	4.5
434969.942(736)	0.0076	-4.9209	22.2451	4	3.5	4.5	3	3.5	3.5
434981.187(736)	0.1117	-3.7547	22.2451	4	3.5	3.5	3	3.5	3.5
434989.954(736)	0.0078	- 4.9103	22.2451	4	3.5	2.5	3	3.5	3.5
434992.515(736)	0.0077	- 4.9191	22.2447	4	3.5	3.5	3	3.5	2.5
435001.282(736)	0.0882	- 3.8576	22.2447	4	3.5	2.5	3	3.5	2.5
441582.376(150)	4.2867	-2.1574	22.0245	4	3.5	4.5	3	2.5	3.5
441582.389(150)	3.1494	-2.2913	22.0241	4	3.5	3.5	3	2.5	2.5
441583.110(150)	2.2857	-2.4305	22.0251	4	3.5	2.5	3	2.5	1.5
441591.156(150)	0.2792	-3.3437	22.0249	4	3.5	2.5	3	2.5	2.5
441593.620(150)	0.2790	-3.3440	22.0245	4	3.5	3.5	3	2.5	3.5
441602.388(150)	0.0058	- 5.0264	22.0245	4	3.5	2.5	3	2.5	3.5
443442.746 (103)	0.0028	-5.3455	22.2455	4	4.5	3.5	3	3.5	4.5
443454.063 (103)	0.2202	- 3.4436	22.2455	4	4.5	4.5	3	3.5	4.5
443457.252(103)	0.2200	- 3.4439	22.2451	4	4.5	3.5	3	3.5	3.5
443467.854(103)	5.3333	- 2.0594	22.2455	4	4.5	5.5	3	3.5	4.5
443468.570(103)	4.2242	- 2.1606	22.2451	4	4.5	4.5	3	3.5	3.5
443468.581(103)	3.3328	- 2.2636	22.2447	4	4.5	3.5	3	3.5	2.5
543514.715(888)	0.1167	-3.5767	37.0380	5	4.5	5.5	4	4.5	5.5
543525.968(888)	0.0040	- 5.0419	37.0380	5	4.5	4.5	4	4.5	5.5
543528.506(888)	0.0039	- 5.0532	37.0376	5	4.5	5.5	4	4.5	4.5
543539.758(888)	0.0932	- 3.6745	37.0376	5	4.5	4.5	4	4.5	4.5
543548.983(888)	0.0040	- 5.0414	37.0376	5	4.5	3.5	4	4.5	4.5
543551.076(888)	0.0039	-5.0507	37.0372	5	4.5	4.5	4	4.5	3.5
543560.301(888)	0.0773	- 3.7558	37.0372	5	4.5	3.5	4	4.5	3.5



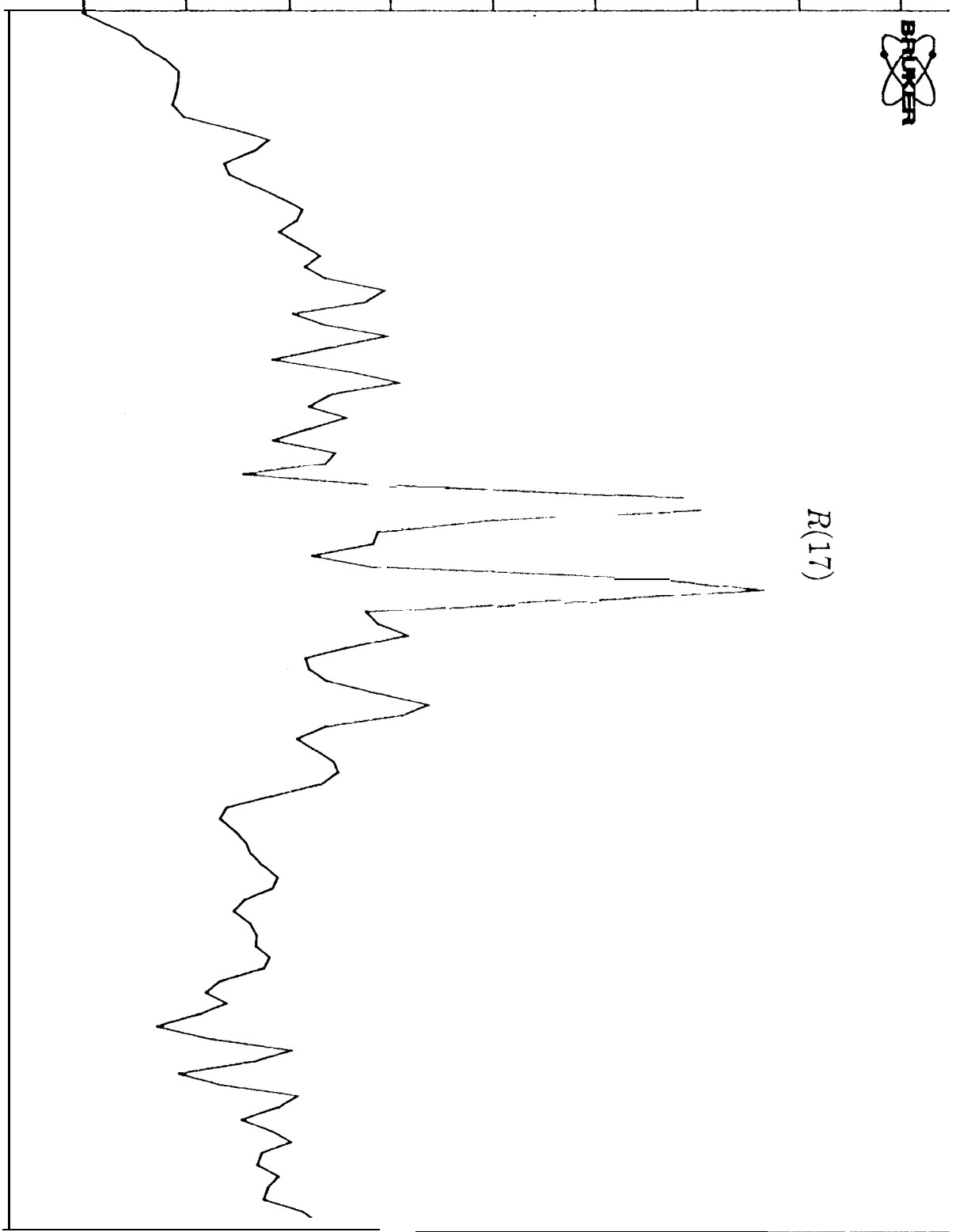


Emission

8.40 8.45 8.50 8.55 8.60 8.65 8.70 8.75 8.80

R(17)

272.824 1272.9 1273.0 1273.1 1273.2 1273.3 1273.378  
Wavenumber cm<sup>-1</sup>



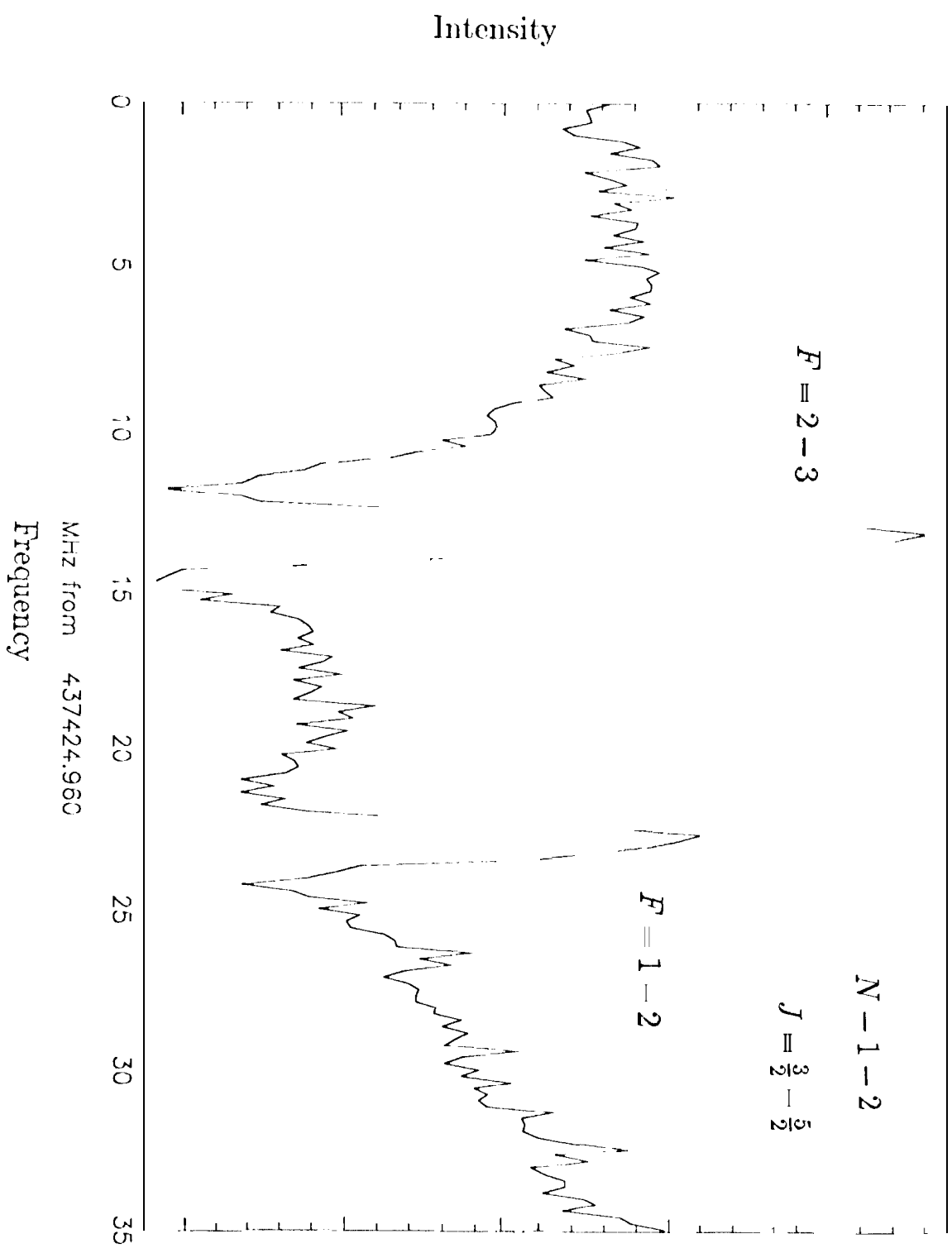


## FIGURE CAPTIONS

### **Figure 1.**

Portion of the infrared emission spectrum of SrH.

The transitions of the free radical appear in emission on the top of a large continuum which originates mostly from the walls of the hot dl.

### **Figure 11.**

Expanded portion of the infrared emission spectrum of SrH.

around the P(9) line of the fundamental band.

The doublet structure of the rotational lines is a result of splitting of the energy levels due to spin-rotation interaction.

### **Figure 111.**

Portion of the rotational spectrum of SrH